Original Article

DOI: 10.5582/bst.2020.01051

Design, synthesis, and biological evaluation of 4-phenoxybenzenesulfonyl pyrrolidine derivatives as matrix metalloproteinase inhibitors

Jing Mao[1], Hao Zhang[1], Xuejian Wang[1], Jianjun Gao[2], Jinbao Tang[1,*], Jian Zhang[1,*]

[1] Department of Medical Chemistry, School of Pharmacy, Weifang Medical University, Weifang, Shandong, China;
[2] Department of Pharmacology, School of Pharmacy, Qingdao University, Qingdao, Shandong, China.

SUMMARY A series of 4-phenoxybenzenesulfonyl pyrrolidine derivatives were designed, synthesized, and evaluated as matrix metalloproteinases (MMPs) inhibitors. All of the synthesized compounds displayed inhibitory activity against MMP-2 and MMP-9. Compounds **4a**, **4e**, and **4i** displayed more potent activity than the other compounds. While the three compounds mildly or moderately inhibited the proliferation of cancer cells, they significantly suppressed the migration and invasion of cancer cells at relatively low concentrations as determined by a wound healing assay and transwell assay. In addition, compound **4e** suppressed vascular endothelial cell tube formation and sprouting of microvessels from aortic rings *in vitro* in a dose-dependent manner. Compound **4e** markedly suppressed the pulmonary metastasis of H22 cells in mice. These findings along with molecular docking results suggested that compound **4e** might be a promising candidate for further structural optimization to develop MMP inhibitors as potential anticancer agents.

Keywords MMP inhibitor, pyrrolidine derivatives, anticancer agent

1. Introduction

Enzymatic proteolysis of cell surface proteins and extracellular matrix (ECM) is critical for tissue homeostasis and cell signaling (*1*). These proteolytic activities are mediated predominantly by a family of structurally and functionally related zinc-dependent endoproteinases termed matrix metalloproteinases (MMPs) (*2*). MMPs are involved in many aspects of physiological processes, as well as in pathologies, such as arthritis, cardiovascular, inflammation, tumor growth, and metastasis (*3-5*). Among more than 25 MMPs, MMP-2 and MMP-9 play an important role in virtually all aspects of cancer progression, making them important therapeutic targets for drug development (*6*).

A number of laboratories have endeavored in recent decades to discover many potent and orally active broad-spectrum MMP inhibitors. Some have reached the stage of an advanced clinical trial, as exemplified by CGS 27023A, prinomastat, and ilomastat (*7,8*). Colleagues of the current authors have previously reported several kinds of synthetic MMP inhibitors, such as caffeoyl pyrrolidine derivatives (*9*), sulfonyl pyrrolidine derivatives (*10*), quinoxalinone peptidomimetic derivatives (*11*), Pro-Gly peptidomimetic derivatives (*12*), and phosphonic 1,4-dithia-7-azaspiro[4,4] nonane derivatives (*13*).

In a previous work, the current authors' group thoroughly studied L-hydroxyproline scaffold-based derivatives as effective MMP inhibitors. Compound LY52 in particular potently inhibited MMP-2 and was found to inhibit tumor invasion and metastasis (*14*). Based on the fact that the sulfonamide group can be incorporated in metalloenzyme inhibitors to improve enzyme-inhibitor binding (*15*), arylsulfonyl pyrrolidine derivatives were designed by the current authors. In those derivatives, the 4-phenoxybenzenesulfonyl group and different aroyl groups are introduced into the trans-S-hydroxy-L-proline scaffold (Figure 1). This article describes the synthesis and evaluation of the biological activity of these MMP inhibitors.

2. Materials and Methods

2.1. Chemicals

Unless otherwise noted, all commercially available starting materials, reagents, and solvents were used without further purification. All reactions were monitored using TLC with 0.25 mm silica gel plates (60GF-254) and visualized with UV light, iodine stain, and ferric chloride. Silica gel or C18 silica gel was used for column chromatography purification. Flash chromatography was performed using the automated CombiFlash Rf system from Teledyne ISCO. ^{1}H NMR

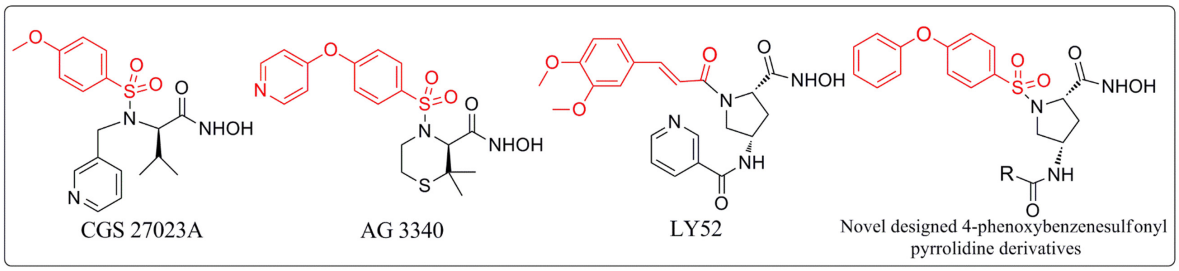

Figure 1. The structures of CGS27023A, AG3340, LY52, and novel designed 4-phenoxybenzenesulfonyl pyrrolidine derivatives.

and ^{13}C NMR spectra were recorded on a Bruker DRX spectrometer at 600 MHz; chemical shifts (d) were recorded in parts per million and the coupling constant (*J*) was measured in Hertz, and TMS served as an internal standard. ESI-MS was performed on an API 4000 spectrometer at the Weifang Medical University Analysis and Test Center in Weifang, Shandong, China.

2.2. *In vitro* MMP-2 and MMP-9 inhibition assay

Recombinant human MMP-2, MMP-9 and the fluorogenic substrate Mca-Pro-Leu-Gly-Leu-Dap(Dnp)-Ala-Arg-NH2 were all purchased from Enzo Life Sciences (Farmingdale, NY, USA). Compounds **4a-i** and the positive control LY52 were assayed for their inhibitory activities against MMP-2 and MMP-9 using the Fluorometric Drug Discovery Kit. Twenty μL of the enzyme solution and 20 μL of the tested compound with different gradient concentrations were added to the 96-well plate. The 100% group contained no inhibitor and the blank group contained no enzyme. After incubation for 45 min at 37°C, 10 μL of the fluorogenic substrate was added to start the reaction, and the resulting solution was measured at 328 nm/420 nm.

2.3. MTT assay

Cell proliferation was determined using an MTT (3-[4, 5-dimethyl-2-thiazolyl]-2, 5-diphenyl-2*H*-tertazolium bromide) assay. Cells were plated on 96-well plates (10000 cells/well) and cultured for 4 hours in RPMI1640 medium containing 10% FBS at 37°C in a 5% CO_2 humidified incubator, and then treated with various concentrations of the tested compounds (with LY52 as the positive control). After incubation for 48 h, 0.5% MTT was added to each well. Four h later, formazan formed by MTT was dissolved with DMSO for 15 min. The OD value was measured using an ELISA reader at 570 nm.

2.4. Colony formation

A549 cells were seeded on 6-well plates at a density of 500 cells/well and treated with the tested compounds at a concentration of 5 μM for 24 hours. After incubation for 2 wks, the cells in each well were washed twice with PBS, fixed with methanol for 15 min, and stained with 0.1% crystal violet for 10 min. Then colonies were photographed and counted under an inverted microscope.

2.5. Wound healing assay

A wound healing assay was performed by plating cells on 6-well culture dishes. After A549 cells were allowed to attach and reach 80% confluence, a scratch (1 mm) was made through the culture dish with a sterile plastic 200 μL micropipette tip to generate one homogeneous wound along each well. After wounding, non-adherent cells were removed and washed twice with PBS. Cells were further incubated without or with the indicated compounds for 48 h and the wound width was measured under a microscope using an ocular grid.

2.6. Transwell assay

Migration and invasion assays were performed on a 24-well plate using a transwell chamber (Darmstadt, Hesse, Germany) with a pore size of 8 microns. Then, 1×10^5 of A549 cells were added to the upper chamber pre-coated with Matrigel (BD Bioscience, Bedford, MA, USA). Each well of cells was seeded with the compound in RPMI 1640 medium containing 1% FBS in the upper chamber. The lower chamber contained 10% FBS as a chemoattractant. After incubation at 37°C for 24 h, the cells were carefully removed from the upper side of the filter with a cotton swab. The membrane was then fixed with methanol for 10 minutes and stained with 0.1% crystal violet, and cells were photographed and counted under an inverted microscope.

2.7. Tube formation assay

A 24-well chamber was coated with 100 μL Matrigel (BD Biosciences, Bedford, MA, USA) and allowed to gel for 30 min at 37°C. Then, 1×10^5 of human umbilical vein endothelial cells (HUVECs) per well were suspended in growth medium without or with increasing concentrations of compound **4e** or LY52. The formation of capillary tubes was identified after incubation for 8 h. Images were captured with an inverted microscope. Tube formation was determined

by counting branch points of the formed tubes, and the average numbers of branch points were calculated.

2.8. Rat thoracic aorta ring (TAR) assay

A 96-well chamber was coated with 100 μL Matrigel (BD Biosciences, Bedford, MA, USA) and allowed to gel for 30 min at 37°C. Thoracic aortas were removed from 6-wk-old male SD rats. After carefully removing the perivascular tissue, the thoracic aorta was roughly cut into a 1-mm-long ring, and each ring was embedded in an independent Matrigel-coated well. Aorta rings were treated every other d with tested compounds for 9 d and photographed on the 10^{th} d at 200× magnification.

2.9. *In vivo* H22 tumor transplant model

In this experiment, Kunming mice were subcutaneously inoculated with 1×10^7/mL murine H22 cells (*16*). Seven d after inoculation with H22 cells, the transplanted mice were randomly divided into four groups with 7 mice per group. The mice were treated with **4e** or LY52 at the specified dose for 5 d/wk for two wks (**4e** Low: 50 mg/kg/d; **4e** High: 100 mg/kg/d; LY52: 50 mg/kg/d). Mice in the blank group were treated with PBS. After 14 d of treatment, mice were sacrificed, and their lungs were fixed with Bouin solution and the number of lung nodules was counted.

2.10. Computational docking assay

A docking study was conducted as follows: the selected compound was constructed with a Sybyl/Sketch module and optimized using the Powell Energetic Gradient method with a Tripos force field with the convergence criterion set at 0.05 kcal/mol Å, and charges were assigned using the Gasteiger-Hückel method. The docking study of the selected compound **4e** with the active site of MMP-2 was performed using the Sybyl/FlexX module. The radius of the active site was 10.0 Å surrounding Zn^{2+} (PDB: 1HOV).

2.11. Statistical analysis

Data were analyzed using one-way analysis of variance (ANOVA) followed by Dunnett's multiple range tests, and data are expressed as the mean ± SD. $p < 0.05$ was considered to indicate a statistically significant difference. Statistical analysis was performed using the software SPSS/Win 16.0 (SPSS, Chicago, USA).

3. Results

3.1. Chemistry

The target compounds were efficiently synthesized following the procedures shown in Scheme 1. The chemical structures of all target compounds are also listed and were analytically confirmed using ^{1}H-NMR and ^{13}C-NMR.

Starting from (2*S*,4*S*)-1-*tert*-butyl-2-methyl-4-aminopyrrolidine-1,2-dicarboxylate (**1**), intermediates (**2a-i**) were prepared *via* a condensation reaction with various aromatic acids or pyridine-3-sulfonic acid and isobutyl chloroformate (IBCF) as a condensation agent and triethylamine (TEA) as a base. After deprotection of the compounds **2a-i** in the presence of hydrogen chloride, the crude products without further purification were treated with 4-phenoxybenzene-1-sulfonyl chloride to yield compounds **3a-i**, which were treated with NH2OK in anhydrous methanol to yield the target compounds **4a-i**. For specific procedures for synthesis and spectroscopic data on all compounds, see Supplementary Data (*http://www.biosciencetrends.*

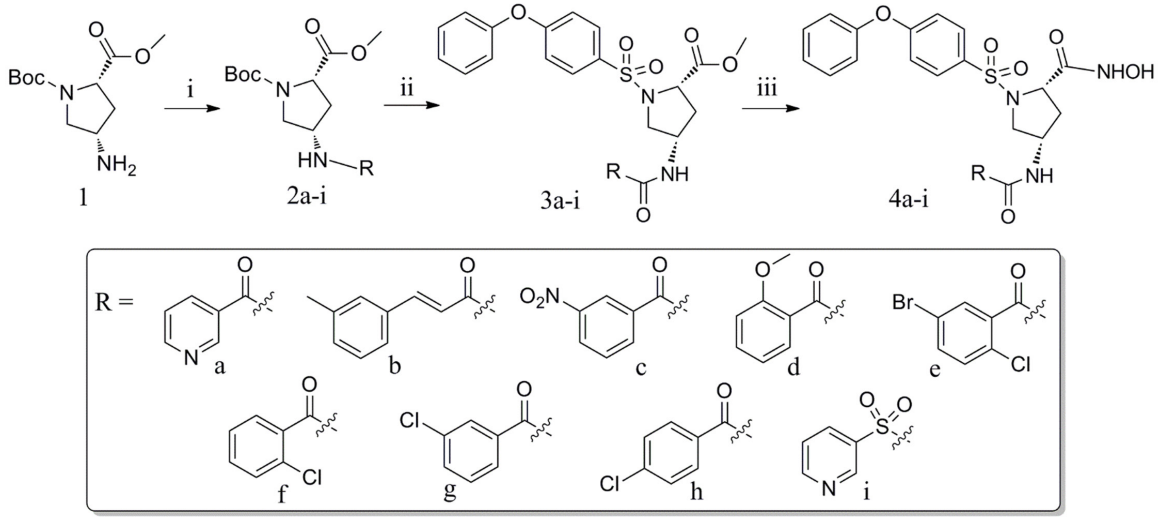

Scheme1. Reagents and conditions. (i) Isobutyl chloroformate, Et_3N, THF; (ii) HCl/EtOAC; 4-phenoxybenzene-1-sulfonyl chloride, DCM, TEA; (iii) NH_2OK, MeOH, 65%.

com/action/getSupplementalData.php?ID=65).

3.2. Suppression of the activity of MMP-2 and MMP-9 by synthesized compounds

The newly synthesized 4-phenoxybenzenesulfonyl pyrrolidine derivatives were assayed for their inhibitory activity against MMP-2 and MMP-9, and LY52 served as the positive control. The inhibition results (IC_{50}) are summarized in Figure 2. Compounds **4a-i** all displayed potent inhibitory activity against MMP-2 and MMP-9. Notably, **4a**, **4e**, and **4i** displayed more potent inhibitory activity against MMP-2 and MMP-9 than the other synthesized compounds and LY52; **4i** in particular displayed the most potent activity at the nanomole level (IC_{50} = 0.05 μM for MMP-2 and 0.08 μM for MMP-9).

3.3. Inhibition of cell growth by compounds **4a**, **4e**, and **4i**

Compounds **4a**, **4e** and **4i** were chosen to evaluate their antiproliferative activity against different tumor cell lines: A549 (lung cancer cells), ES-2 (ovarian clear cell carcinoma cells), Hela (human cervical carcinoma cells), K562 (chronic myelogenous leukemia cells), and MDA-MB-231 (human breast adenocarcinoma cells). LY52 served as a positive control. Results are shown in Figure 3A. Compound **4e** displayed the most potent activity against the proliferation of cancer cells among the tested compounds. To confirm the anti-growth activity of the tested compounds, a colony formation assay was performed to measure the effect of **4a**, **4e**, and **4i** at a concentration of 5 μM in A549 cells. As shown in Figures 3B and 3C, compound **4e** was superior to other compounds in suppressing clone formation by A549 cells.

3.4. Suppression of cell migration and invasion by compounds **4a**, **4e**, and **4i**

The activity of compounds **4a**, **4e**, and **4i** on the migration of A549 cells was assessed using a wound

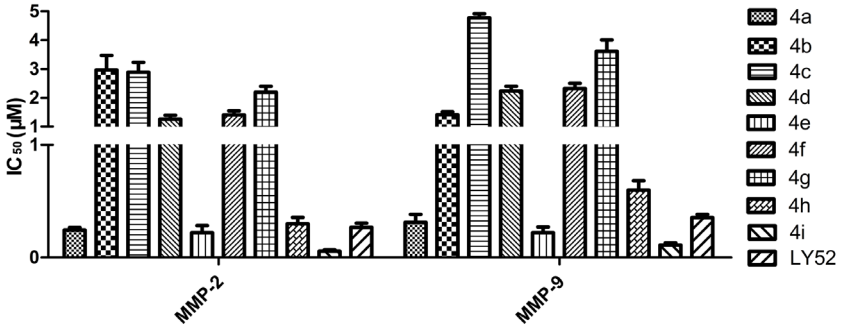

Figure 2. The inhibitory activities of the target compounds (4a-4i) against MMP-2 and MMP-9.

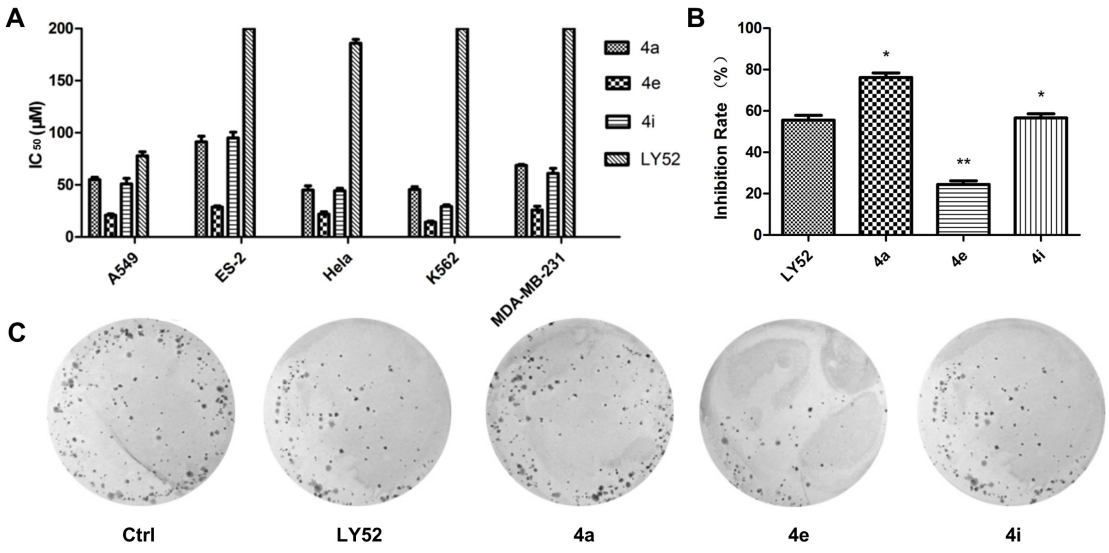

Figure 3. Inhibitory effects of 4a, 4e, and 4i on the growth of cancer cells. (A) IC_{50} values for **4a**, **4e**, and **4i** in A549, ES-2, Hela, K562, and MDA-MB-231 cells as determined by an MTT assay. **(B and C)** Inhibitory effect of **4a**, **4e**, and **4i** on clone formation of A549 cells. The rate of inhibition was estimated by counting the number of colonies containing > 50 cells, $^{*}p < 0.05$ *vs.* control; $^{**}p < 0.01$ *vs.* control.

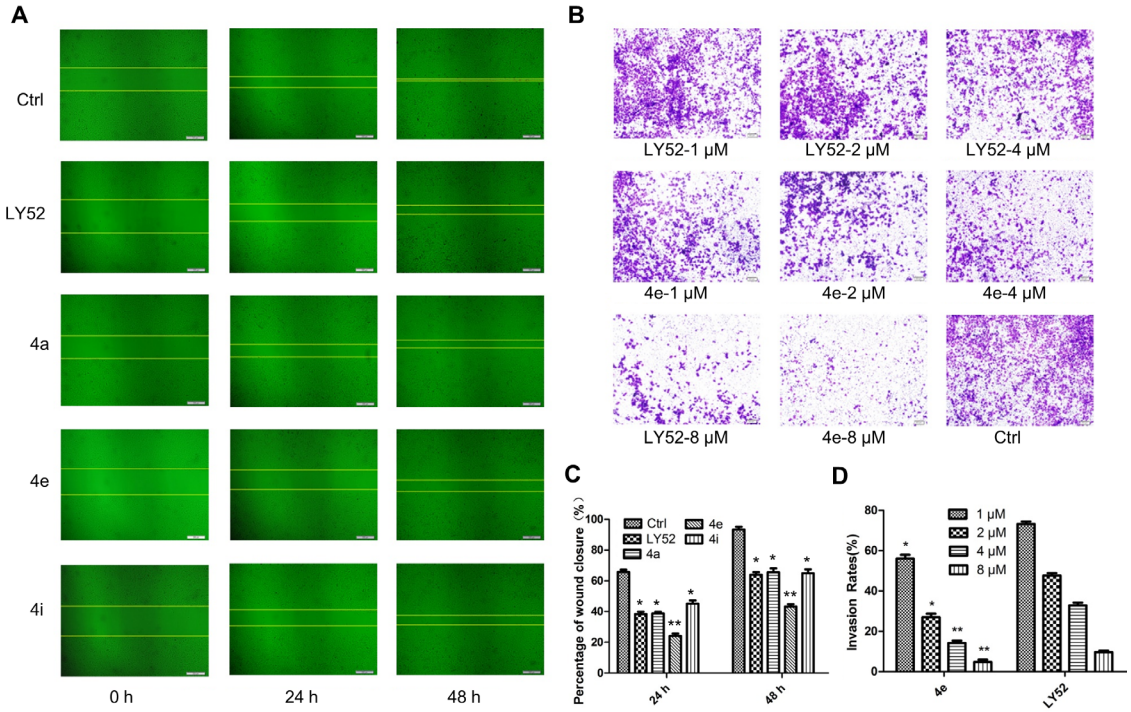

Figure 4. Inhibitory effects of 4a, 4e, and 4i on the migration and invasion of A549 cells as determined by a wound healing assay (A and C) and transwell assay (B and D). Cells were treated with **4a**, **4e**, or **4i** at a concentration of 5 μM for 48 h in a wound healing assay. Cells were treated with **4e** at incremental concentrations for 24 h. $^{*}p < 0.05$ *vs.* control; $^{**}p < 0.01$ *vs.* control.

healing assay. The concentration of all of the tested compounds was 5 μM. As shown in Figures 4A and 4C, compounds **4a**, **4e**, and **4i** markedly suppressed the migration of A549 cells as reflected by delayed wound closure. Compound **4e** was superior to other compounds in delaying wound closure. The anti-invasive activity of compound **4e** was evaluated using a transwell assay. Results indicated that it markedly reduced the number of invading cells in a dose-dependent manner (Figures 4B and 4D).

3.5. Suppression of angiogenesis by compound **4e** *in vitro*

To study its anti-angiogenesis action, compound **4e** was first evaluated for its cytotoxicity against HUVECs. Compound **4e** displayed relatively low cytotoxic activity with an IC_{50} of 22.42 μM. A HUVEC tube formation assay was then performed *in vitro* with **4e** and LY52 at concentrations of 1, 2, 4, and 8 μM. Results in Figure 5 indicate that **4e** reduced the number of branch points of HUVECs in a dose-dependent manner and almost completely inhibited tube formation at a concentration of 8 μM. Compared to HUVEC tube formation, the rat TAR model more closely resembles *in vivo* conditions during the process of angiogenesis. Compound **4e** was evaluated for microvessel formation at different concentrations (1, 2, 4, and 8 μM). Results indicated that the number of microvessels sprouting from aortic rings was significantly decreased by **4e** in a dose-dependent manner (Figure 6).

3.6. Suppression of cancer metastasis by compound **4e** *in vivo*

Treatment of A549 cells with compound **4e** at a concentration of 8 μM markedly decreased cancer cell migration and invasion *in vitro*. Encouraged by this finding, together with the potent anti-angiogenesis effects of **4e** *in vitro*, its anti-metastasis activity was examined in a H22 pulmonary metastasis model *in vivo*. As shown in Figures 7A and 7B, there were much fewer metastatic pulmonary nodes in mice treated with **4e** than in the LY52 group. Mice treated with **4e** did not experience any discernible adverse reactions or significant changes in body weight during the experiment.

3.7. Molecular docking results

Compound **4e** was chosen for a docking study to investigate its binding mode at the active site of MMP-2 (PDB: 1HOV). Results in Figure 8A suggest that the hydroxamic acid group can chelate with catalytic Zn^{2+} and that the 4-phenoxybenzenesulfonyl group can enter the S1' pocket, while the bromo- and chloro- substituted benzoyl group can occupy the S2' pocket. For a detailed understanding of the interactions of **4e** with the residues along the active site of the protein, a diagram of H-bond interactions was created (Figure 8B). The hydroxyl group and imido group of hydroxamic acid can form hydrogen bonds with Glu^{121} and the carbonyl group can form hydrogen bonds with His^{130}.

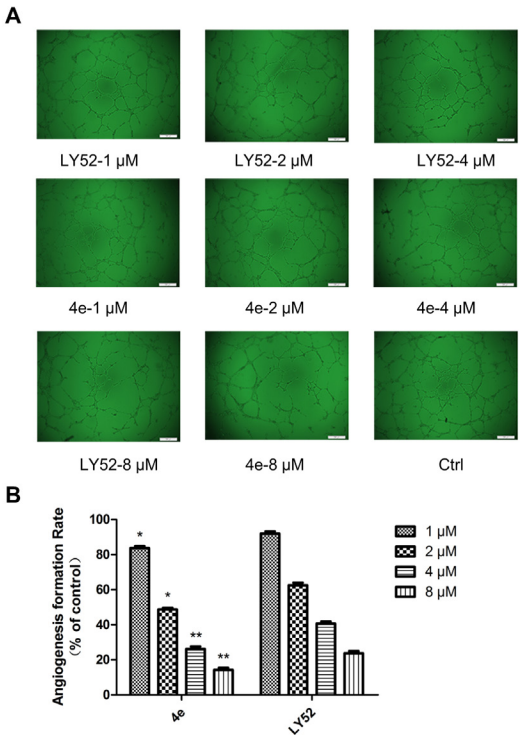

Figure 5. Compound 4e suppressed vascular endothelial cell tube formation *in vitro*. HUVECs were incubated with the indicated concentrations of **4e** or **LY52** for 8 h. The images were captured with an inverted microscope. Tube formation on Matrigel was determined by counting the branch points of formed tubes. $^{*}p < 0.05$ *vs.* control; $^{**}p < 0.01$ *vs.* control.

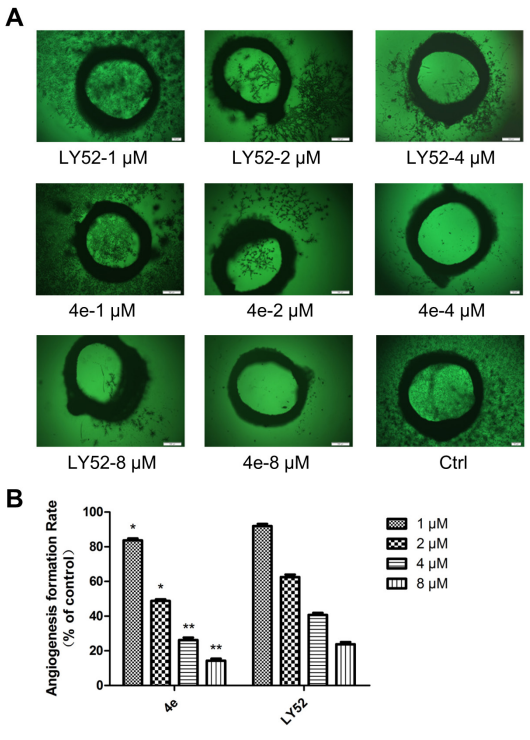

Figure 6. Compound 4e suppressed sprouting of microvessels from aortic rings. Thoracic aortas excised from 6-wk-old male SD rats were treated every other d with **4e** or **LY52** for 9 d and photographed on the 10th d at 200 × magnification. $^{*}p < 0.05$ *vs.* control; $^{**}p < 0.01$ *vs.* control.

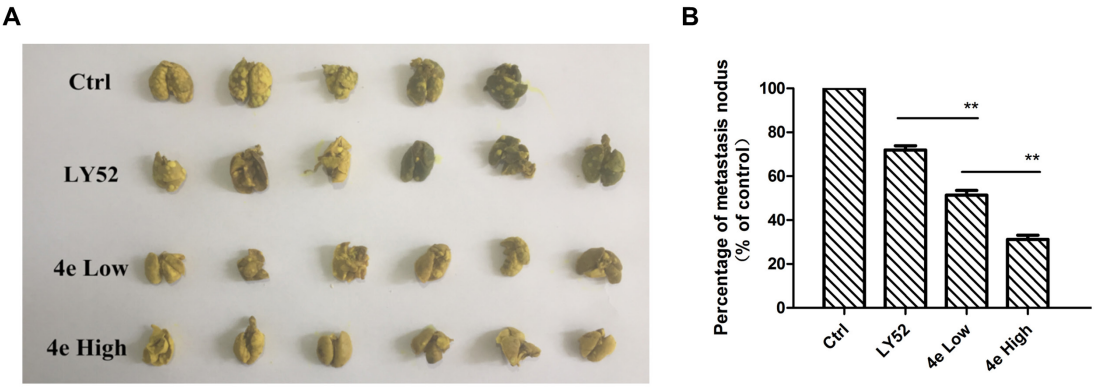

Figure 7. Compound 4e reduced metastatic pulmonary nodes in mice. Mice that were inoculated subcutaneously with H22 cells were treated with **4e** or **LY52** at the specified dose for 5 d/wk for two wks. At the end of experiment, the lungs were removed and fixed with Bouin solution and the number of lung nodules was counted. $^{*}p < 0.05$ *vs.* control; $^{**}p < 0.01$ *vs.* control.

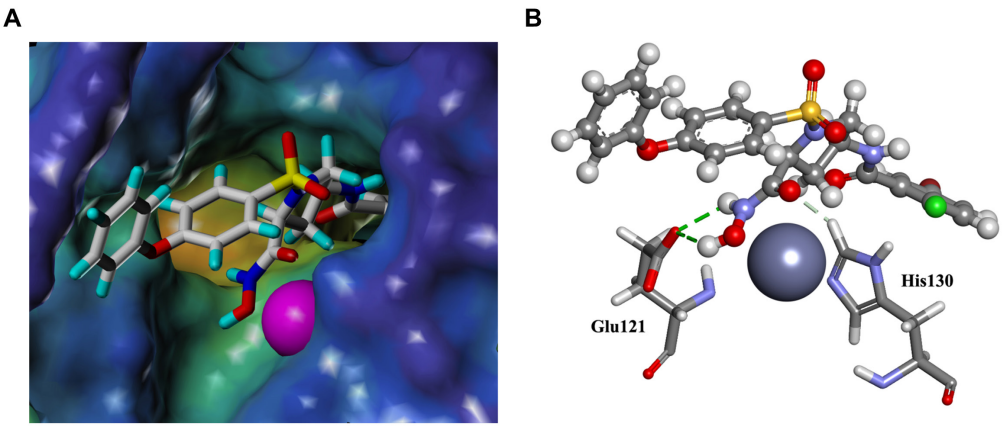

Figure 8. The FlexX docking (A) and binding mode (B) of compound 4e with MMP-2.

4. Discussion

Reported here is the synthesis and biological evaluation of 4-phenoxybenzenesulfonyl pyrrolidine derivatives as MMP-2/MMP-9 inhibitors. All of the synthesized compounds displayed potent inhibitory activity against MMP-2/MMP-9; **4a**, **4e**, and **4i** were more potent than the other compounds. These compounds' ability to suppress cell proliferation, migration, and invasion, angiogenesis *in vitro*, and cancer metastasis *in vivo* were also examined. Results suggested that the target compounds have a mild or moderate inhibitory effect on cancer cell proliferation. However, they significantly suppressed cell migration and capillary tube formation at low concentrations *in vitro*. Compound **4e** also significantly suppressed the metastasis of H22 cells in mice. These results suggest that the novel 4-phenoxybenzenesulfonyl pyrrolidine derivatives synthesized in this study have the potential to suppress cancer metastasis.

This study investigated the structure-activity relationship (SAR) of all target compounds. There is no obvious subtype selectivity between MMP-2 and MMP-9 for these 4-phenoxybenzenesulfonyl pyrrolidine derivatives. Among compounds **4c-h** containing a substituted benzoyl group, the bromo- and chloro-substituted compound **4e** had more potent inhibitory activity. Chloro- or methoxy- substitution at the *ortho* position of the benzoyl group results in no marked differences in inhibitory activity, but the *p*-chloro-substituted compound **4h** displayed more potent inhibitory activity. Among the synthesized compounds, compound **4i** containing a 3-pyridine-sulfonamide group displayed the most potent activity against MMP-2 and MMP-9. This result might be due to the contribution of electronegative nitrogen atoms, which can more easily form hydrogen bonds with the enzyme backbone, thus stabilizing the bond between the compound and the enzyme. However, results indicated that the anti-proliferative and anti-migration activity of **4i** was not superior to that of **4e**. Linking the enzyme-inhibiting activity of MMPs with their cellular potency is difficult because several other variables should be considered, such as cellular membrane permeability, metabolic stability, subcellular localization, and cellular xenobiotic export. There is also a possibility that compound **4e** has other targets involved in cell proliferation and migration, so further study is warranted.

In conclusion, the current study synthesized a series of 4-phenoxybenzenesulfonyl pyrrolidine derivatives as MMP-2/MMP-9 inhibitors. Representative compound **4e** inhibited the proliferation, migration, angiogenesis, and metastasis of cancer cells. These results indicate that **4e** is a promising candidate for further structural optimization and evaluation to develop MMP inhibitors in the future.

Acknowledgements

This work was supported by the Natural Science Foundation of Shandong Province (Grant No. ZR2019QH015), the National Natural Science Foundation of China (Grant No. 80813368), and the Higher Educational Science and Technology Program of Shandong Province (Grant No. J17KB098).

References

1. Jabłońska-Trypu A, Matejczyk M, Rosochacki SA. Matrix metalloproteinases (MMPs), the main extracellular matrix (ECM) enzymes in collagen degradation, as a target for anticancer drugs. J Enzyme Inhib Med Chem. 2016; 31:177-183.
2. Scherer RL, McIntyre JO, Matrisian LM. Imaging matrix metalloproteinases in cancer. Cancer Metastasis Rev. 2008; 27:679-690.
3. Bäck M, Ketelhuth DF, Agewall S. Matrix metalloproteinases in atherothrombosis. Prog Cardiovasc Dis. 2010; 52:410-428.
4. Hu J, Van den Steen PE, Sang QX, Opdenakker G. Matrix metalloproteinase inhibitors as therapy for inflammatory and vascular diseases. Nat Rev Drug Discov. 2007; 6:480-498.
5. Egeblad M, Werb Z. New functions for the matrix metalloproteinases in cancer progression. Nat Rev Cancer. 2002; 2:161-174.
6. Overall CM, Kleifeld O. Tumour microenvironment-opinion: Validating matrix metalloproteinases as drug targets and anti-targets for cancer therapy. Nat Rev Cancer. 2006; 6:227-239.
7. Rajeshwar PV, Corwin H. Matrix metalloproteinases (MMPs): Chemical-biological functions and (Q)SARs. Bioorg Med Chem. 2007; 15:2223-2268.
8. Tu GG, Xu WF, Huang HM, Li SH. Progress in the development of matrix metalloproteinase inhibitors. Curr Med Chem. 2008; 15:1388-1395.
9. Li YL, Xu WF. Design, synthesis, and activity of caffeoyl pyrrolidine derivatives as potential gelatinase inhibitors. Bioorg Med Chem. 2004; 12:5171-5180.
10. Cheng XC, Wang Q, Fang H, Tang W, Xu WF. Design, synthesis and evaluation of novel sulfonyl pyrrolidine derivatives as matrix metalloproteinase inhibitors. Bioorg Med Chem. 2008; 16:5398-5404.
11. Li YG, Zhang J, Xu WF, Zhu HW, Li X. Novel matrix metalloproteinase inhibitors derived from quinoxalinone scaffold (Part I). Bioorg Med Chem. 2010; 18:1516-1525.
12. Zhang J, Li XY, Jiang YQ, Feng JH, Li XG, Zhang YJ, Xu WF. Design, synthesis and preliminary evaluation of α-sulfonyl γ-(glycinyl-amino) proline peptidomimetics as matrix metalloproteinase inhibitors. Bioorg Med Chem. 2014; 22:3055-3064.
13. Zhang H, Li X, Wang XJ, Xu WF, Zhang J. Sulfonyl phosphonic 1,4-dithia-7-azaspiro[4,4]nonane derivatives as matrix metalloproteinase inhibitors: Synthesis, docking study and biological evaluation. Drug Discov Ther. 2017; 11:118-125.
14. Qu XJ, Yuan YX, Xu W.F, Chen MH, Cui SX, Meng H, Li YL, Makuuchi M, Nakata M, Tang W. Caffeoyl

pyrrolidine derivative LY52 inhibits tumor invasion and metastasis *via* suppression of matrix metalloproteinase activity. Anticancer Res. 2006; 26:3573-3578.
15. Cheng XC, Wang Q, Fang H, Xu WF. Roles of sulfonamide group in matris metalloproteinase inhibitors. Curr Med Chem. 2008; 15:368-373.
16. Jiang YQ, Li XY, Hou JN, Huang YX, Wang XJ, Jia YP, Wang QW, Xu WF, Zhang J, Zhang YJ. Synthesis and biological characterization of ubenimex-fluorouracil conjugates for anti-cancer therapy. Eur J Med Chem. 2018; 143:334-347.

Received February 20, 2020; Revised April 26, 2020; Accepted April 27, 2020.

**Address correspondence to:*
Jian Zhang and Jinbao Tang, Department of Medical Chemistry, School of Pharmacy, Weifang Medical University, 7166 West Baotong Road, Weifang, Shandong, China 261053.
E-mail: zhangjian_3323@163.com (JZ), tangjinbao2002@126.com (JT)

Released online in J-STAGE as advance publication May 9, 2020.